Analysis of aerosol characteristics over the China Sea by remote sensing

DENG Xueliang[1, 3], HE Dongyan[2], PAN Delu[3], SUN Zhaobo[4]

1. *Key Laboratory of Atmospheric Science and Satellite Remote Sensing*, *Anhui Institute of Meteorology*, *Anhui Hefei* 230031, *China*;
2. *Anhui Climate Centre*, *Anhui Hefei* 230061, *China*;
3. *State Key Laboratory of Satellite Ocean Environment Dynamics*, *Second Institute of Oceanography*, *State Oceanic Administration*, *Zhejiang Hangzhou* 310012, *China*;
4. *Nanjing University of Information Science & Technology*, *Jiangsu Nanjing* 210044, *China*

Abstract: MODIS Collection 005(MODIS_C005) aerosol product is validated over the China Sea. Aerosol optical thickness at 550nm (AOT550) and fine mode fraction (FMF) are used to analyze spatial-temporal distribution of aerosol over the China Sea. Then meteorological data are used to discuss formation mechanism of aerosol characteristics. The results show that firstly MODIS_C005 aerosol product has a good quality over the China Sea. Secondly, AOT550 and FMF have a notable spatial-temporal distribution feature. AOT550 reaches maximum in spring and winter, and minimum in summer and fall; oppositely, FMF reaches maximum in summer and fall, and minimum in spring and winter. Meanwhile, AOT550 and FMF have marked longitudinal variation. AOT550 appears maximum between 30°N—40°N and decreases towards north and south. And FMF increases from south to north and the tendency of increase becomes slow at 30°N. In addition, they have an obvious meridional variation. AOT550 and FMF both decrease with the increase of longitude. Finally, based on meteorological data, the source is the continent aerosol and wind and rainfall are the two most important factors.

Key words: China Sea, aerosol, spatial-temporal distribution, formation mechanism

CLC number: TP79/P407 **Document code:** A

Citation format: Deng X L, He D Y, Pan D L and Sun Z B. 2010. Analysis of aerosol characteristics over the China Sea by remote sensing. *Journal of Remote Sensing*. **14**(2): 294—312

1 INTRODUCTION

Atmospheric aerosol is usually defined to be liquid or solid suspended particles with a diameter smaller than 10μm (Zhang, 1995). Tropospheric aerosol is an important part of earth-atmosphere-ocean system, which effects radiation budget by direct forcing and indirect forcing so as to influences global climate and environment, so aerosol is a crucial factor in global climatic fluctuations (Patadia *et al.*, 2008).

Researches of climatologists showed that climatic fluctuations may be closely associated with aerosol, such as the cooling of Sichuan province (Li *et al.*, 1995) and precipitation pattern of south flood and north drought in China (Menon *et al.*, 2002). Increased atmospheric stability and decreased precipitation in east China may be related with high aerosol density and large aerosol absorption (Zhao *et al.*, 2006), which suggests that aerosol act upon regional and global climate by its radiative forcing.

China offing is the main fishery region and an important part in China climate system, so understanding the distribution of aerosol over the China Sea is of great significance for national economy. Aerosol over the China Sea has obvious mixed characteristic, including marine aerosol and continental aerosol, so it is very complex. In order to explain its feature, many scientists have done much research. Aerosol optical thickness (AOT) is measured by sun photometer over the Yellow Sea (Li *et al.*, 2003). AOT is 0.2—0.4 in clear sky, while it is markedly increasing to 0.8 under atmospheric haze over the Yellow Sea and East China Sea (Zhao *et al.*, 2005).

Though a lot of vessel surveys, preliminary characteristic of aerosol distribution can be known. But because of small time scale and swift spatial variation of aerosol, ship-based measurement can not meet aerosol observe requirement which is long time scale and great spatial region. Since 1990, Scientists began to analyze aerosol by remote sensing. Aerosol distribution over the North Africa is studied by MIRS data (Christopher *et al.,* 2008). Aerosol radiative forcing is analyzed over global ocean by remote sensing (Bellouin *et al.*, 2008). Aerosol distribution over the China Sea is discussed by SeaWiFS data (Hao *et al*., 2007).

Received: 2008-07-29; **Accepted**: 2008-12-18

Foundation: State Key Laboratory of Satellite Ocean Environment Dynamics (Grant No.SOED0911); Anhui Provincial Natural Science Foundation (Grant No.090415216); Wuhan Regional Meteorologic Center (Grant No.QY-Z-200902).

First author biography: DENG Xueliang (1981—), male, doctor. He got doctor degree from Nanjing University of Information Science & Technology in 2008, now researches on marine aerosol. E-mail: dengxueliang9989@yahoo.com.cn

In this paper we present aerosol distribution by MODIS aerosol product and discuss the reason with weather data.

2 STUDY AREA AND DATA

The study region is between 10°N—50°N and 110°E—150°E, including the China Sea. The area of study and Aerosol Robotic Network (AERONET) stations is shown in Fig. 1. The data sets include MOD04_L2, AERONET data and NCEP reanalysis data. These data are acquired for the period between December 2000 and December 2006.

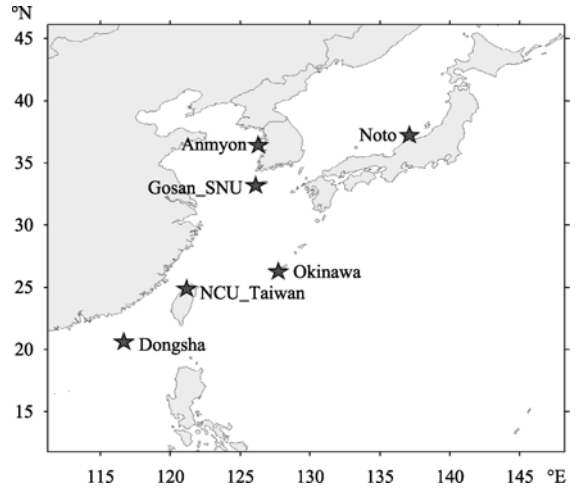

Fig. 1 Research area and AERONET stations

2.1 MODIS aerosol product

The second-generation MODIS aerosol retrieval (Collection 005) from EOS-Terra (2000—2006) have been used in this study. This new version is released during 2007 (Remer & Kaufman, 2005) and modification has been made in the algorithm to improve the aerosol data product.

Aerosol optical thickness (AOT) expresses atmospheric turbidity and aerosol concentration, which is an crucial factor in aerosol climate effect and atmosphere model. The higher aerosol concentration is, the larger AOT (Zhang, 2007).

Fine mode fraction (FMF) is defined as the fraction of the total optical thickness attributed to the selected fine mode (diameter < 1μm) as Eq. (1). The higher FMF is, the larger fraction of fine mode aerosol, and vice versa. Anthropogenic aerosol is almost fine mode such as sulfate and natural aerosol is always large mode such as dust and sea salt, so FMF can distinguish anthropogenic component and natural component from aerosol.

$$\tau = \frac{\tau_{550,\text{fine}}}{\tau_{550}} \tag{1}$$

2.2 AERONET database

AERONET is a federation of well calibrated ground based sun-photometers that provide spectral AOT and other aerosol properties from hundreds of locations around the world. The cloud-cleared level 2.0 data was used from 4 stations for 2000—2004 (Fig. 1). The estimated uncertainty in AERONET AOT is about 0.01—0.02 (Holben *et al*., 1998). The program provides a long-term, continuous and readily accessible public domain database of aerosol optical, mircrophysical and radiative properties for aerosol research and characterization, and validation of satellite retrievals. Aerosol optical depth data are computed for three data quality levels: Level 1.0 (unscreened), Level 1.5 (cloud-screened), and Level 2.0 (cloud-screened and quality-assured). AERONET data were compared against the MODIS AOT values for 2000—2004. It is not the purpose of this paper. This only prepares data validation for analysis of aerosol distribution over the China Sea.

2.3 NCEP/NCAR Reanalysis data

Monthly mean, 850hp wind speed and direction, and rainfall data were obtained from National Centers for Environmental Prediction (NCEP) Reanalysis data. NCEP Reanalysis contains meteorological conditions with a 2.5 degree horizontal resolution at 6h time intervals.

3 MODIS COLLECTION005 AOT VALIDATION

MODIS Collection005 AOT has not been validated over the China Sea, so firstly it must be validated before analyzing aerosol distribution. Hiren *et al*. (2007) prove that MODIS Collection 005 AOT has better quality than Collection 004, compared with AERONET data at Kanpur, India. Now this is not found over the China Sea.

AOT550 derived from MODIS and AERONET must be matched on space and time. Window size on space and time are set as 50km×50km and 1h in the anterior research. But Larger window size could introduce undesirable errors due to topographic or aerosol type heterogeneity, so three space box size (30km×30km, 50km×50km and 70km×70km) have been compared. The result shows that 30km×30km box can improve validation effect and expresses aerosol regional characteristic.

AERONET stations are showed in Fig.1, which represent different sea areas. Fig.2 shows the scatter plots of MODIS AOT550 against AERONET AOT550 in different stations over the China Sea. The correlation and regression coefficients show excellent agreement with AERONET measurements over the China Sea (Fig. 2(a)—Fig. 2 (e)). Meanwhile, the relationship in Fig.2 are all good and their correlation coefficients are greater than 0.9. The largest value reaches 0.9662 at Noto and correlation coefficient of total stations is 0.9307. Errors of 65% points are under $\pm 0.05 \pm 0.05\tau$ based on NASA standard (62%), so MODIS AOT550 is fit to the China Sea and can be used to research aerosol distribution over the China Sea (Cheng, 2005). FMF is validated over the ocean (Anderson, 2005; Remer, 2005), whose error is about 20%.

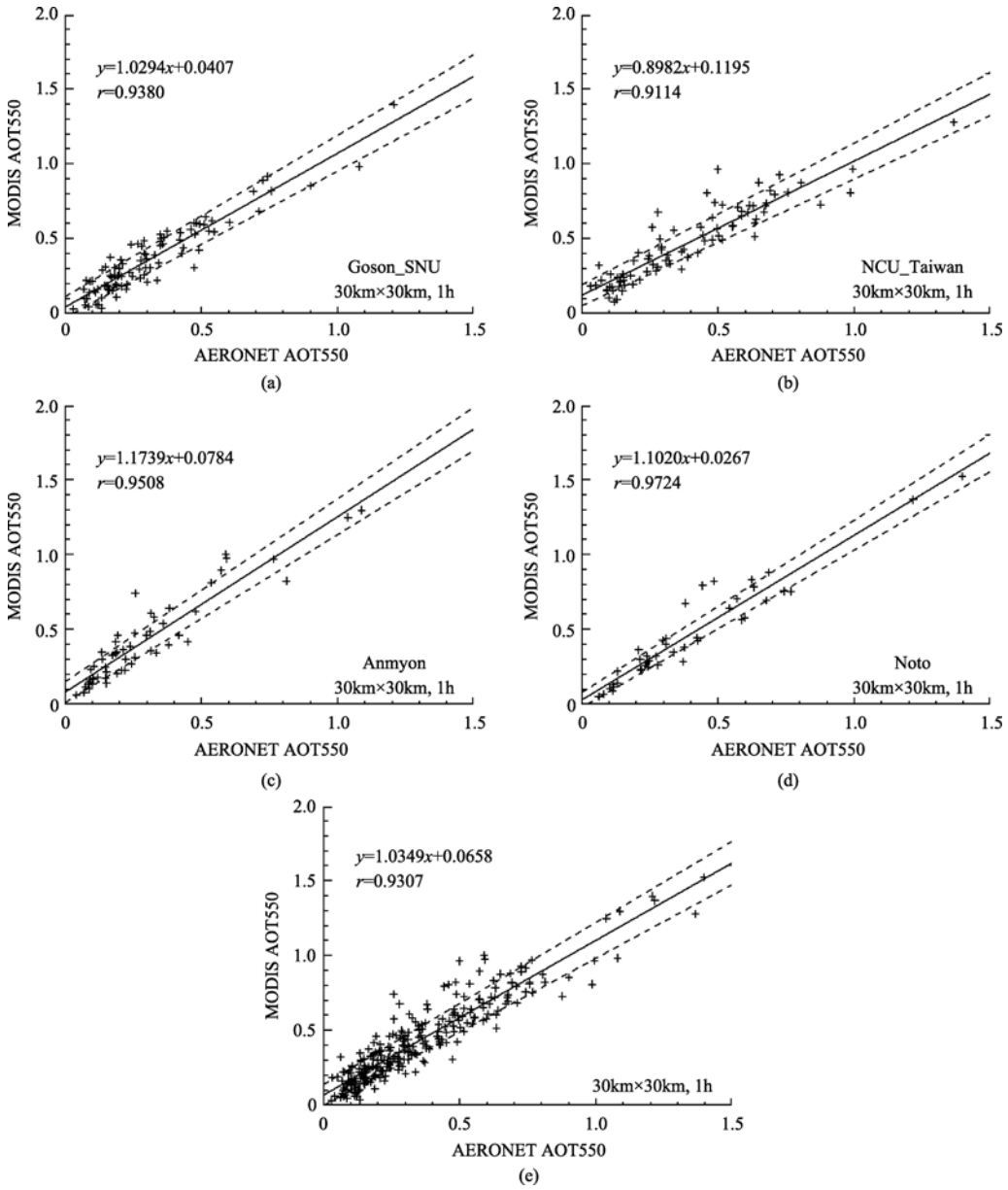

Fig. 2 Scatter plot between AOT550 derived from MODIS and AERONET from 2001 to 2004 with their corresponding equations and correlation coefficients in different sites over the China Sea

(a) Gosan_SNU; (b) NCU_Taiwan; (c)Anmyon; (d) Noto; (e) Sum of the 4 sites

4 RESULTS AND DISCUSSIONS

4.1 Temporal variation

4.1.1 Seasonal change

Fig.3 shows six years mean spatial distribution of MODIS AOT550 in different seasons over the China Sea. AOT550 has notable seasonal change. Maximum AOT550 appears in spring. Minimum AOT550 is in summer. In winter, distribution of AOT550 is along the coast. AOT550 decreases obviously with increase in distance far from continent. Maximum AOT550 has been observed in coastal region and the value of it is larger than 0.5, meanwhile, minimum AOT550 appears in open ocean and value of it is 0.1. AOT550 around 30°N reaches maximum, where human activity is active. AOT550 over the north of 25°N is all larger than 0.17 and it over the south of 25°N is smaller than 0.17. In spring, distribution pattern of AOT550 is similar with it in winter. Because of dust prevailing, AOT550 increases obviously and is all larger than 0.17 over the whole China Sea. In summer, distribution pattern of AOT550 changes remarkably. AOT550 is large in the north of the China Sea and is small in the south. Maximum appears over the Yellow Sea and Bohai

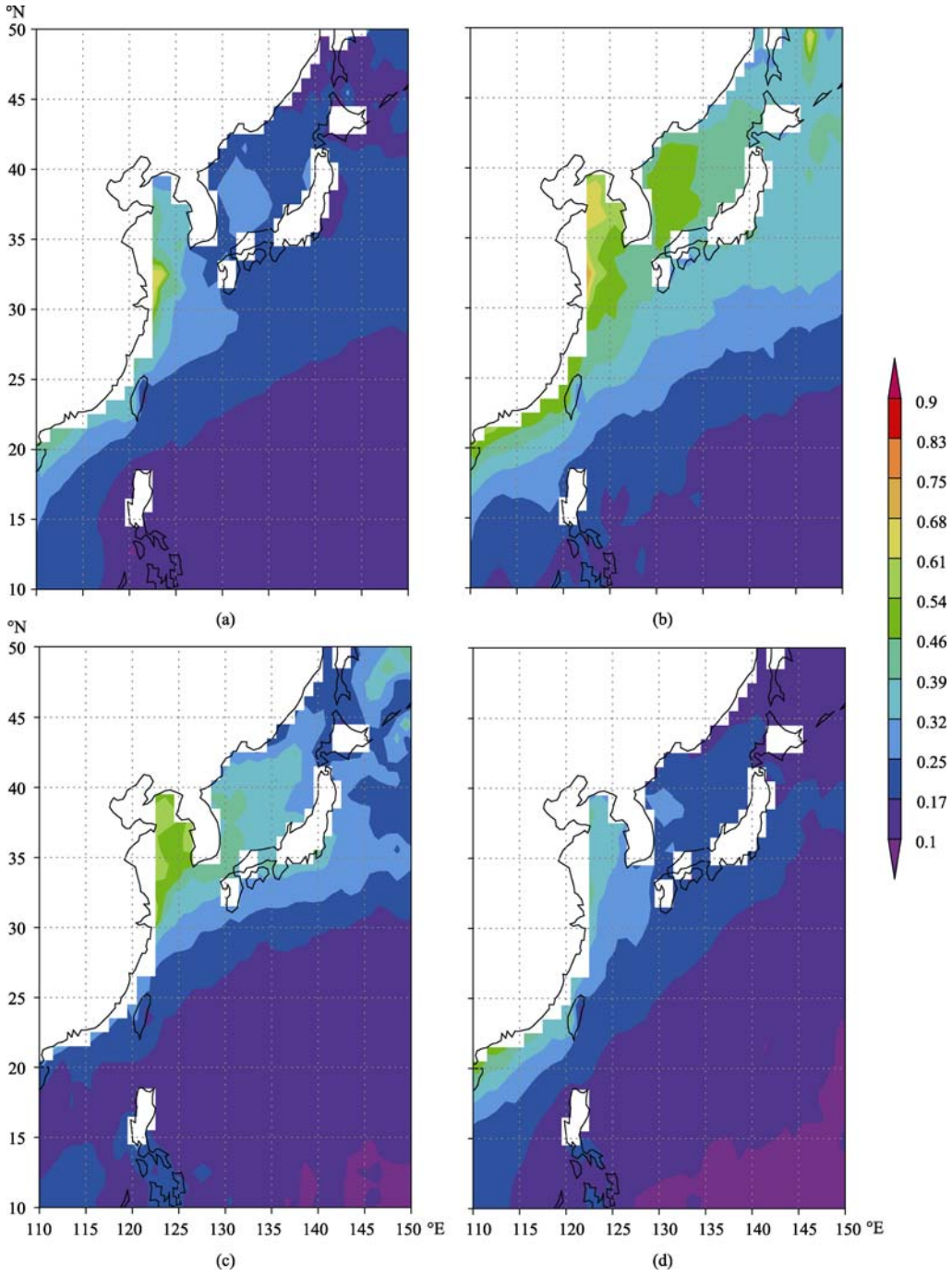

Fig. 3 Seasonal distribution of AOT550 over the China Sea
(a) Winter; (b) Spring; (c) Summer; (d) Fall

Sea. Value of AOT550 becomes the least in four seasons. In fall, the pattern of AOT550 returns to the one in winter.

Fig.4 shows six years mean spatial distribution of MODIS FMF in different seasons over the China Sea. FMF also has an obvious seasonal change as AOT550. Maximum FMF appears in summer and Minimum FMF is in spring. In winter, distribution pattern of FMF is similar as AOT550. Isoline is related with distance far from the coast. Regions with high FMF is coast and region of low FMF is open sea, which suggests that human activity influences aerosol scale. In spring, FMF has similar pattern while it increased over the sea area of Philippines and Japan due to frequent human events. In summer, FMF has a distinct feature, which is the largest in the north and the least in the south. Maximum value appears over the Yellow Sea and Bohai Sea when FMF is larger than 0.8. In fall, the pattern returns to the one in winter.

4.1.2 Time list

Fig.5 shows time list of monthly area mean AOT550 and

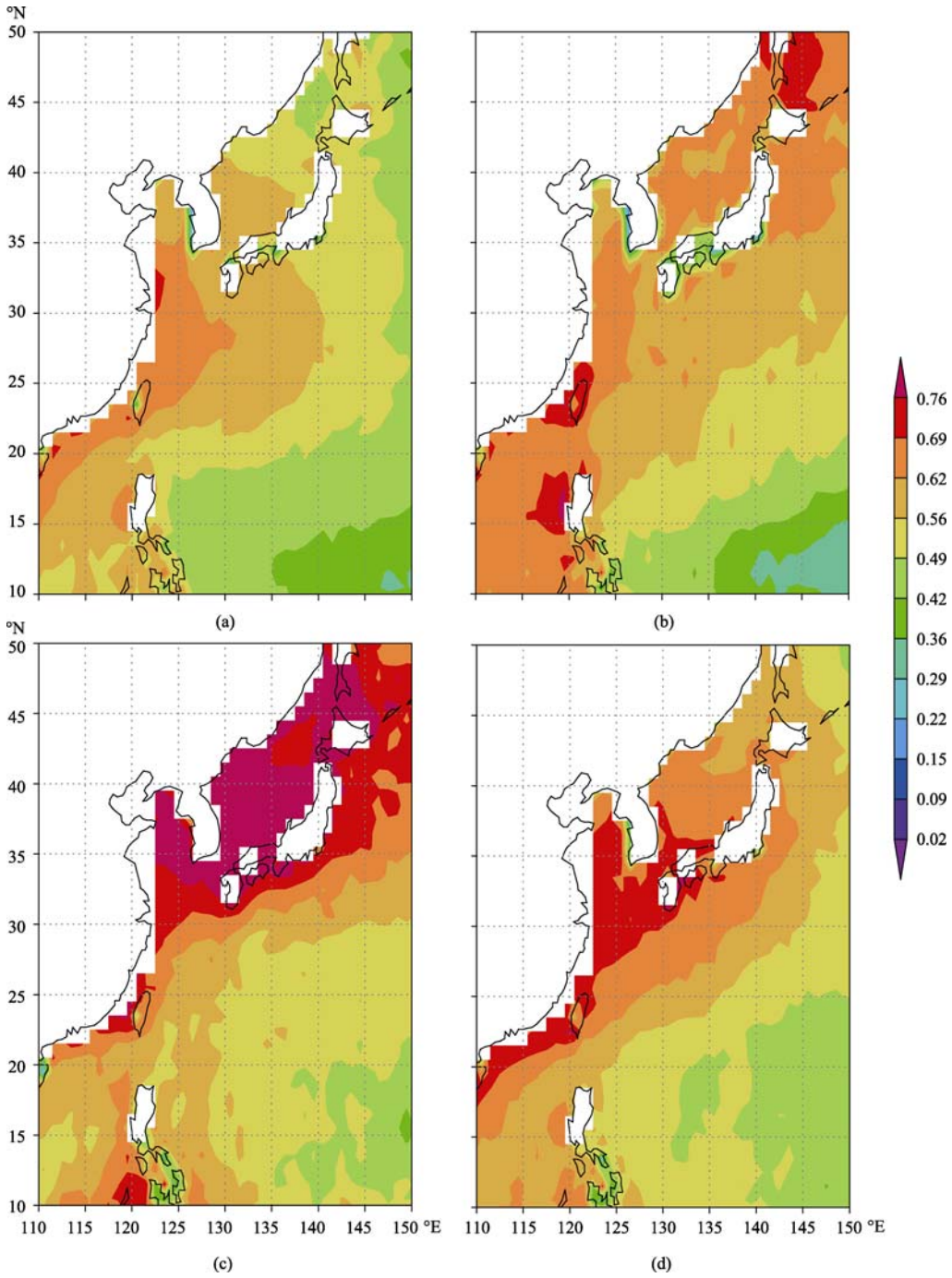

Fig. 4 Seasonal distribution of FMF over the China Sea
(a) Winter; (b) Spring; (c) Summer; (d) Fall

FMF from 2000 to 2006 over the China Sea. AOT550 and FMF over the China Sea exists a clear periodic variety and has an annual cycle. Firstly, AOT550 appears maximum in spring and it is almost larger than 0.4. On the contrary, AOT550 reaches minimum in summer and it is less than 0.25. Similarly, FMF also has a periodic oscillation. But the tendency of FMF is opposite to AOT550. FMF reaches maximum in summer and it is almost larger than 0.6. In the meantime, FMF gets minimum in spring and it is less than 0.5.

Fig.6 shows month variety of six years (2000—2006) area mean AOT550 and FMF over the China Sea. It also proves the temporal tendency of them. AOT550 is largest in April and is least in September. At the opposition, FMF is largest in September and is least in April.

Based on the above analysis, we can find that AOT550 and FMF does exist significant temporal variety over the China Sea. There is an annual cycle of them and seasonal change is obvious.

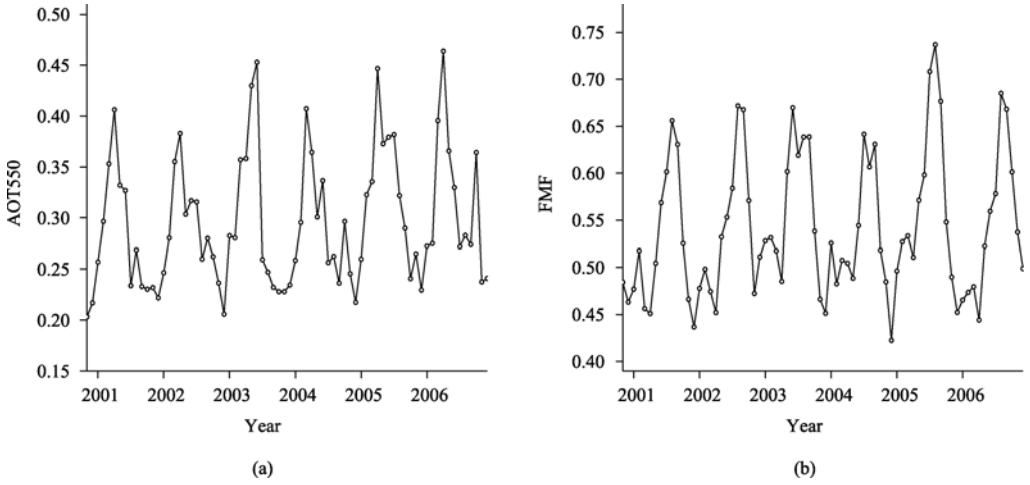

Fig. 5 Time list of region average over the China Sea
(a) AOT550; (b) FMF

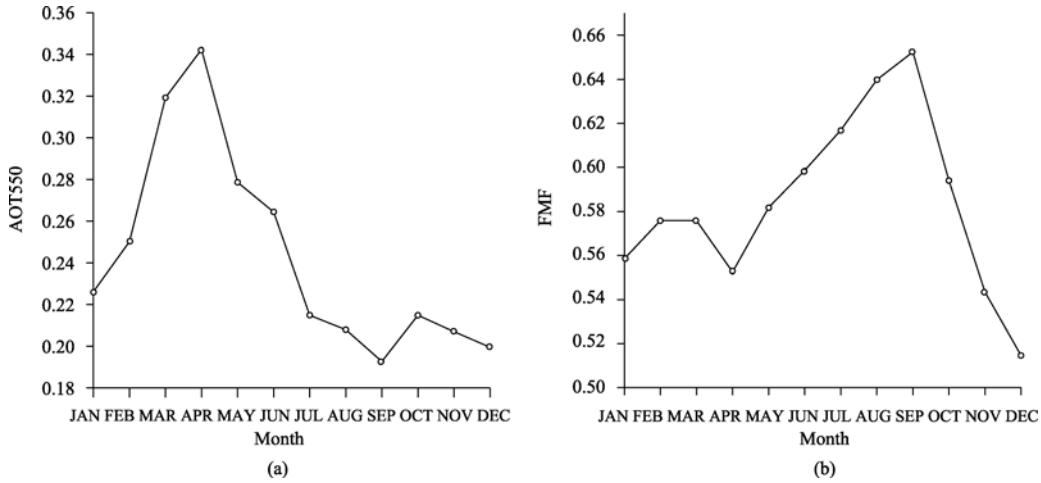

Fig. 6 Month list of region average over the China Sea
(a) AOT550; (b) FMF

4.2 Spatial variation

Besides temporal variety, AOT550 and FMF over the China Sea also exists prominent spatial pattern. Because aerosol over the China Sea is mainly influenced by continent source, it represents a spatial characteristic related with the distance far from the coast and important industry regions. Fig.7 shows latitude-time and longitude-time diagrams of AOT550 and FMF over the China Sea. Fig.8 shows spatial distribution of six years mean AOT550 and FMF along longitude and latitude direction.

Firstly, at latitude direction, there are main industry regions between 30°N and 40°N, so AOT550 appears the highest value. At the same region, FMF also reaches the highest value. However, on the south 30°N, due to lack of industry pollution, AOT550 and FMF both get less and less. In six years mean situation (Fig.8), spatial characteristic of aerosol is much more remarkable. In latitude direction, AOT550 is highest between 30°N and 40°N and decreases towards north and south. FMF gradually increases from south to north.

Secondly, at longitude direction, anthropic influence is very evident. China coast is around 120°E, at the same longitude AOT550 is highest. And AOT550 gradually decrease away from the coast. FMF has the similar pattern. In Fig.8, AOT550 decreases from west to east. Maximum value appears at the coast and minimum value is in the remote ocean. FMF has the same tendency as AOT550. The decrease tendency of AOT has an affinity with the distance far from the continent, which suggests AOT over the East China Sea should be influenced by continental sources and long-range aerosol transport.

Aerosol spatial distribution over the China Sea is very prominent. Continental source may be an important factor for aerosol over the China Sea. The reason of these features will be discussed in the below.

4.3 Reason analysis

The East China is an important aerosol source in the world,

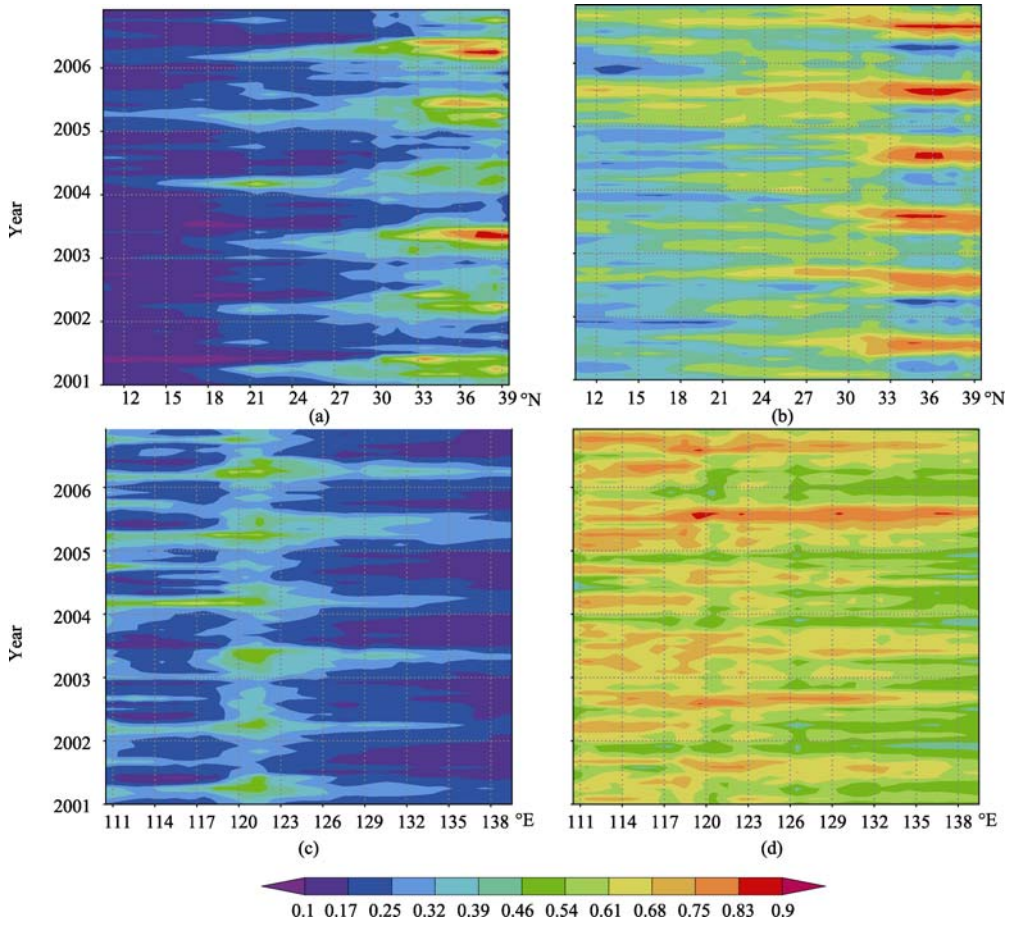

Fig. 7 Meridional and longitudinal distribution of AOT550 and FMF over the China Sea

(a) Longitudinal distribution of AOT550; (b) Longitudinal distribution of FMF; (c) Meridional distribution of AOT550; (d) Meridional distribution of FMF

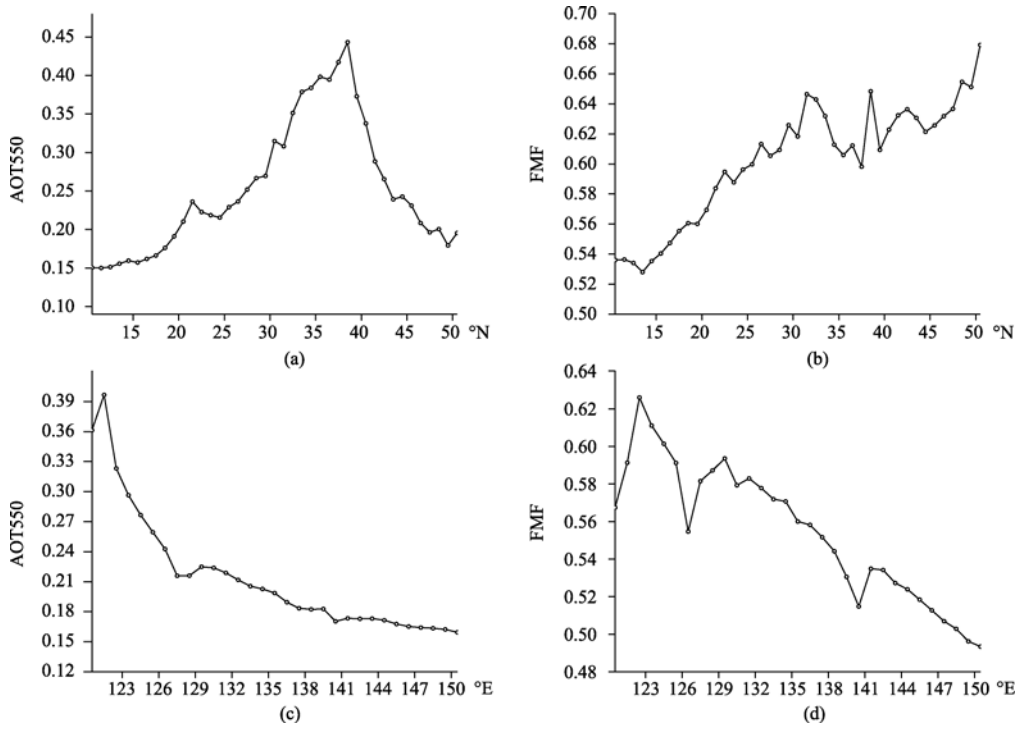

Fig. 8 Meridional and longitudinal distribution of AOT550 and FMF averaged by six years over the China Sea.

(a) Longitudinal distribution of AOT550; (b) Longitudinal distribution of FMF; (c) Meridional distribution of AOT550; (d) Meridional distribution of FMF

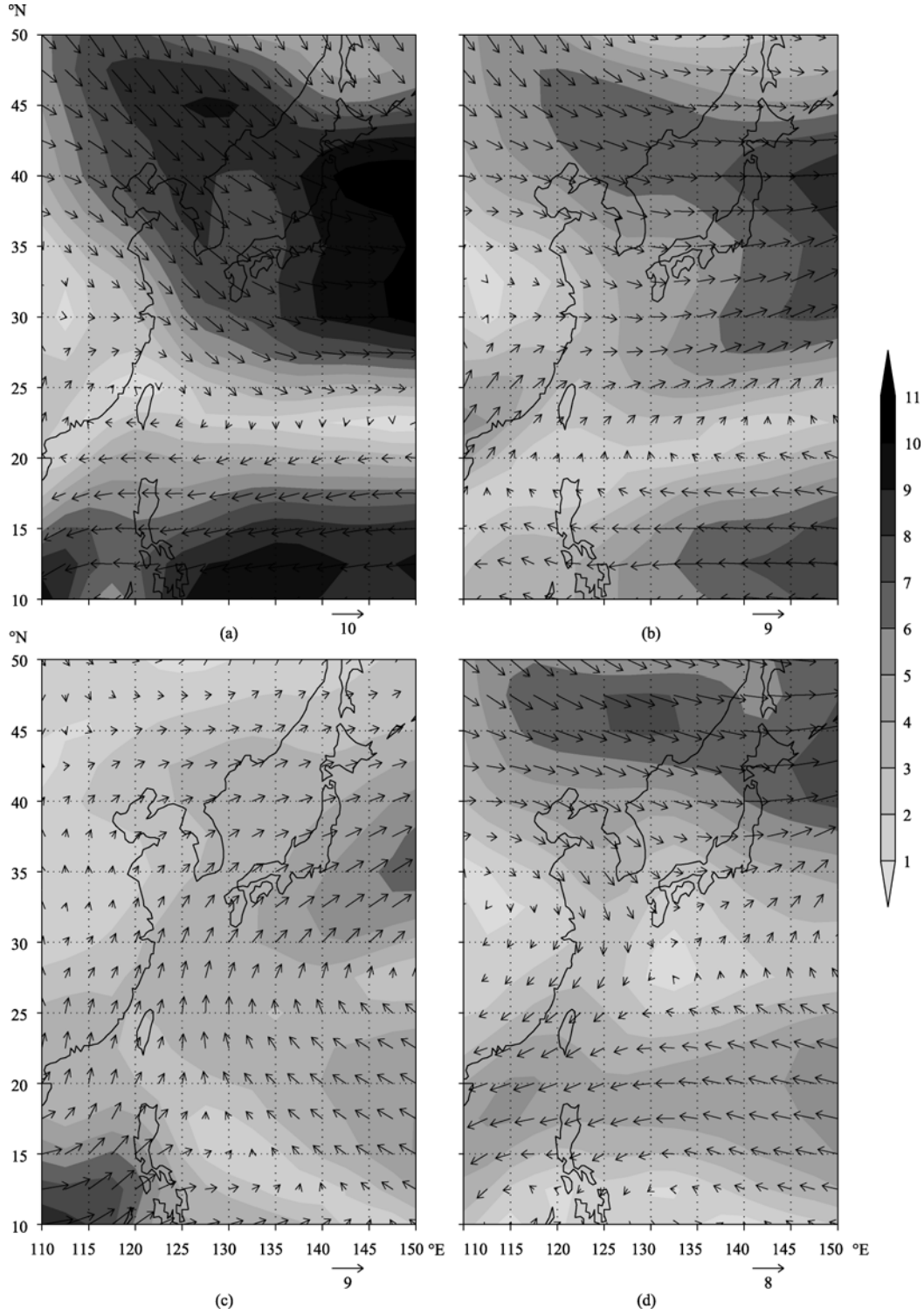

Fig. 9 Sesonal distribution of wind field at 850hp over the China Sea(2000—2006)

(a) Winter; (b) Spring; (c) Summer; (d) Fall

so it must influence the China Sea. Continental aerosol is carried to the China Sea. But aerosol's transport depends on wind, so seasonal change of wind maybe lead to the spatial and temporal distribution pattern of aerosol over the China Sea. Fig.9 shows distribution of mean wind field at 850hp averaged from 2000—2006. There are the similar patterns in winter and spring that northwestern wind control the north of 20°N and eastern wind control the south of 20°N. In summer and fall, eastern wind prevails at most of region, while southwestern wind exist between 30°N—40°N. Meanwhile, rainfall is the highest in summer and fall and is the least in winter and spring. Meteorological condition can effect aerosol distribution.

In winter, continental aerosol is brought to sea region by northwestern wind. High wind speed over the ocean causes that

aerosol is carried and not bank up onto the China Sea, so AOT is not the largest during the year. Besides, big particles of marine aerosol are created by big wind, which lead to the smallest FMF. In spring, dust aerosol is carried to the China Sea by northwestern wind and wind speed becomes weaker than in winter, so aerosol builds up onto the China Sea. AOT reach maximum value and FMF is little due to dust particles. In summer, wind direction changes very visibly. East wind prevails, so continental aerosol can not be transported onto the sea. And rainfall in summer is the largest, big particle aerosol is almost brought down by rain. So AOT is the least and FMF is the largest. In fall, wind field changes. The north of 30°N is controlled by west wind, so AOT550 is larger than summer. Rainfall in fall is next below in summer, so FMF in fall is smaller than in summer, but larger than the other seasons. Based on the above analysis, meteorological condition plays an important role on distribution of AOT and FMF.

5 CONCLUSION

(1) MODIS Collection 005 AOT has a good quality compared with AERONET data and fits NASA standard over the China Sea, so it can be used about the study of the China Sea.

(2) AOT550 and FMF have a notable temporal variation over the China Sea. AOT550 reaches maximum in spring and winter, and minimum in summer and fall; oppositely, FMF reaches maximum in summer and fall, and minimum in spring and winter. Meanwhile, AOT550 and FMF have marked periodic oscillation of one year.

(3) AOT550 and FMF have an obvious spatial distribution over the China Sea. At latitude direction, AOT550 appears maximum between 30°N—40°N and decreases towards to north and south. And FMF increase from south to north and the tendency of increase becomes slow at 30°N. At longitude direction, AOT550 and FMF both decrease with longitude increasing.

(4)Based on meteorological data, wind and rainfall are the two most important factors. Continent aerosol is carried to the China Sea by wind.

Acknowledgements: The authors would like to thank MODIS science data support team for processing level 2 and level 3 data, and AEROENT PIs for collecting aerosol observations around the world.

REFERENCES

Anderson T L, Wu Y and Chu D A. 2005. Testing the MODIS satellite retrieval of aerosol fine-mode fraction. *J. Geophys. Res*., **110**: 182—193

Bellouin N, Jones A and Haywood J. 2008. Updated estimate of aerosol direct radiative forcing from satellite observations and comparison against the Hadley Centre climate model. *J. Geophys. Res*., **113**: 1043—1546

Cheng B Q and Yang Y M. 2005. Validation of MODIS aerosol optical thickness in the Taiwan Strait and its circumjacent sea area. *Acta Oceanologica Sinica*, **27**(6): 170—176

Christopher S A, Gupta P and Haywood J. 2008. Aerosol optical thicknesses over North Africa: 1. Development of a product for model validation using qzone monitoring instrument, multiangle imaging spectroradiometer, and aerosol robotic Network. *J. Geophys. Res*., **113**: 1446—1457

Hao Z Z, Pan D L and Bai Y. 2007. Characteristics of the spatial distribution and monthly variation of aerosol optical thickness derived from SeaWiFS over the China Sea. *Journal of Marine Sciences*, **25**(1): 80—87

Hiren J, Satheesh S K and Srinivasan K. 2007. Assessment of second-generation MODIS aerosol retrieval(Collection 005) at Kanpur, India. *Geophysical Research Letter*, **34**: 1902—1918

Holben B N, Eck T F and Slutsker I. 1998. AERONET-A federated instrument network and data archive for aerosol characterization. *Remote Sensing of Environment*, **66**: 1—16

Li X W, Zhou X J and Li W L. 1995. The cooling of Sichuan province in recent 40 years and its probable mechanism. *Acta Meteorologica Sinica*, **9**: 57—68

Li Z Q, Zhao F S and Zhao W. 2003. Ground surface observationof aerosol optical thickness over Yellow Sea region. *Chinese Journal of Quantum Electronics*, **20**(5): 635—640

Menon S, Hansen J and Nazarenko L. 2002. Climate effects of black carbon aerosols in China and India. *Science*, **297**: 2250—2253

Patadia F, Gupta P and Christopher S A. 2008. First observational estimates of global clear sky shortwave aerosol direct radiative effect over land. *Geophys. Res. Lett*., **35**: 348—360

Remer L A. 2005. The MODIS aerosol algorithm, products and validation. *J. Atmos. Sci*., **62**: 947—973

Remer L A and Kaufman Y. 2005. Didier Tanre. Collection 005 change summary for MODIS aerosol(04_L2) algorithms. USA: NASA

Zhang C C and Zhou W X. 1995. The Lecture of Atmospheric Aerosol. Beijing: China Meteorological Press

Zhang X Y. 2007. Aerosol over China and their climate effect. *Advances in Earth Science*, **22** (1): 12—16

Zhao C S, Tie X X and Lin Y P. 2006. A possible positive feedback of reduction of precipitation and increase in aerosols over eastern central China. *Geophys. Res. Lett*., **33**: 118—132

Zhao W, Tang J W and Gao F. 2005. Measurement and study of aerosol optical properties over the Huanghai Sea and the East China Sea in the spring. *Acta Oceanologica Sinica*, **27**(2): 46—53

卫星遥感中国海域气溶胶特征分析

邓学良[1,3]，何冬燕[2]，潘德炉[3]，孙照渤[4]

1. 安徽省气象科学研究所，安徽省大气科学与卫星遥感重点实验室，安徽 合肥 230031;
2. 安徽省气候中心，安徽 合肥 230061;
3. 卫星海洋环境动力学国家重点实验室，国家海洋局 第二海洋研究所，浙江 杭州 310012;
4. 南京信息工程大学 大气科学学院，江苏 南京 210044

摘 要： 利用 AERONET 地基观测，验证 MODIS Collection5 (MODIS_C005)气溶胶产品在中国海域的适用性。利用其 550nm 气溶胶光学厚度(AOT550)和小颗粒比例(Fine Mode Fraction, FMF)对中国海域气溶胶分布进行分析，结合气象场对其形成机制进行探讨，结果表明：首先，MODIS_C005 气溶胶产品在中国海域有很高精度，适用中国海域；其次，中国海域 AOT550 与 FMF 存在明显的时空分布特征。时间上，AOT550 在冬、春季最大，在夏、秋季最小; FMF 在夏、秋季最大，冬、春季最小。空间上，在经向上, AOT550 在 30°N—40°N 达到最大，向南北递减; FMF 从南向北逐渐增加，到达 30°N 附近后增加减弱。在纬向上, AOT550 和 FMF 随着经度的增加而减小；最后，中国海域气溶胶主要来自于陆源气溶胶，借助风场传输到达中国海域，同时还受到降雨的影响。

关键词： 中国海域，气溶胶，时空分布，形成机制

中图分类号： TP79/P407 **文献标识码：** A

引用格式: 邓学良，何冬燕，潘德炉，孙照渤. 2010. 卫星遥感中国海域气溶胶特征分析，遥感学报. **14**(2): 294—312
Deng X L, He D Y, Pan D L and Sun Z B. 2010. Analysis of aerosol characteristics over the China Sea by remote Sensing. *Journal of Remote Sensing*. **14**(2): 294—312

1 引 言

大气气溶胶通常是指悬浮在大气中直径小于 10μm 的液态或固态的微小粒子(章澄昌 & 周文贤, 1995)。对流层气溶胶是陆地—大气—海洋系统的重要组成部分。它通过直接或间接辐射强迫影响着地—气系统的辐射收支平衡，进而影响全球环境和气候，是气候变化研究的一个重要因子(Patadia 等, 2008)。研究认为中国区域气候变化的一些特点与气溶胶有密切关系，如四川盆地气温下降(Li 等, 1995), 20 世纪 80 年代以来中国“南涝北旱”的降水变化格局(Menon 等, 2002), 中国东部地区大气稳定程度增加，降水减少，这些现象与中国高气溶胶浓度且吸收较高有关(Zhao 等, 2006)。研究表明，气溶胶通过直接和间接辐射强迫在区域乃至全球气候变化中发挥着重要作用。

中国近海是中国主要的海洋渔业区，也是影响中国气候的重要区域，弄清这个海域的气溶胶的分布状况，对于中国国民经济具有重要的意义。由于这个海区的气溶胶不仅具有海洋气溶胶的特点，而且受到陆源输送的影响，具有明显的混合特性，情况复杂。为了弄清中国海域气溶胶的分布特性，近年来很多科学家作了大量的工作。李正强等(2003)利用多波段太阳辐射计测量黄海海域的气溶胶光学厚度。赵崴等(2005)研究发现，春季无云情况下黄海、东海上空的气溶胶光学厚度在 0.2—0.4，海区上空霾层较厚时测量得到的气溶胶光学厚度明显增大，最大接近 0.8。

通过大量航次的调查数据分析，可以初步了解中国海域的气溶胶的分布。由于气溶胶时间尺度很

收稿日期：2008-07-29；修订日期：2008-12-18

基金项目：卫星海洋环境动力学国家重点实验室开放研究基金项目 (编号: SOED0911)；安徽省自然科学基金项目 (编号: 090415216)；武汉区域气象中心科技发展基金项目 (编号: QY-Z-200902)。

第一作者简介：邓学良 (1981—)，男，博士，2008 年博士毕业于南京信息工程大学大气科学学院，目前主要从事海洋气溶胶研究。E-mail: dengxueliang9989@yahoo.com.cn。

小，空间变化很快，船测数据无法满足长时间大面积的气溶胶观测，从 20 世纪 90 年代开始，科学家使用卫星数据对气溶胶进行分析。Christopher 等(2008)利用 MISR 数据分析了北非的气溶胶分布特征。Bellouin 等(2008)利用卫星数据估计了气溶胶的辐射强迫。郝增周等(2007) 利用 SeaWiFS 卫星数据分析了中国海域气溶胶的变化特征。本文利用 MODIS_C005 气溶胶产品对中国海域的气溶胶分布特征和形成机制进行了分析。

2 研究区域和数据

本文研究区域选定为中国海域及其周边海域(10°N—50°N, 110°E—150°E)，图 1 为研究区域以及 AERONET 验证站点。数据选取了 MODIS 气溶胶数据、AERONET 观测数据和 NCEP/NCAR 月平均再分析资料。

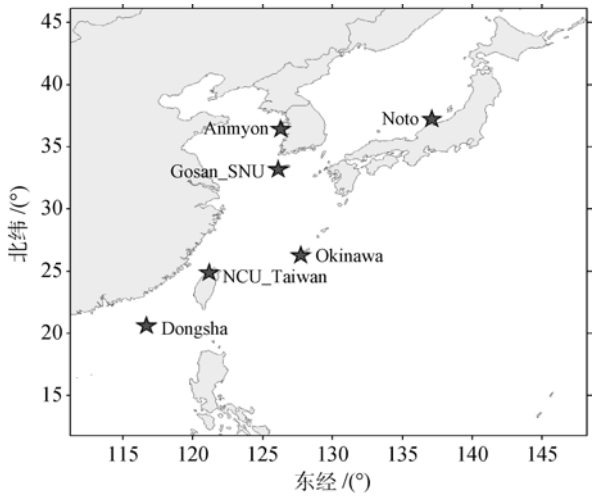

图 1 研究区域和 AERONET 地基站点分布 (星星)

2.1 MODIS 气溶胶产品

收集 2000—2006 年 MODIS_C005 的 Terra/ MOD04_L2 气溶胶产品，包括 AOT550 和 FMF。MODIS_C005 气溶胶产品(Remer & Kaufman, 2005)是 NASA 对 1996 年开始使用的气溶胶反演算法(ATBD-96)进行重新改进后得到气溶胶产品，是对以前使用的 MODIS_C004 数据的进一步完善。气溶胶光学厚度(AOT)是表征大气混浊度和气溶胶含量的一个重要物理量,也是确定气溶胶气候效应的一个关键因子和大气模型的一个重要参量,气溶胶含量越高,则 AOT 的值越大(张小曳，2007)。小颗粒比例(Fine Mode Fraction, FMF)是 MODIS 新的气溶胶参数，定义为 550nm 处小于 1.0μm 的小颗粒气溶胶光学厚度与总气溶胶光学厚度的比例，计算如式(1)。FMF 越大，则小颗粒气溶胶的比例越大; FMF 越小，则小颗粒气溶胶的比例越小。由于人为形成的气溶胶如硫酸盐等，主要是小颗粒气溶胶；而自然气溶胶如沙尘和海盐，主要是大颗粒气溶胶。所以 FMF 还可以用来区分人为气溶胶和自然气溶胶。这对于分析中国海域气溶胶的颗粒分布和形成原因有很大的帮助。

$$\tau = \frac{\tau_{550,\mathrm{fine}}}{\tau_{550}} \tag{1}$$

2.2 AERONET 观测数据

选取了 2001—2004 年中国海域 4 个 AERONET 站点的 level2.0 数据。AERONET 是以美国宇航局 NASA 为首建立的全球气溶胶光学特性监测网络，目的是利用地基太阳光度计获取全球具有代表性区域的探测气溶胶光学特性参数的基准资料，用于验证和评估卫星反演的气溶胶光学特性参数的精度，其精度为 0.01—0.02(Holben 等, 1998)，常用来验证卫星气溶胶光学厚度遥感结果。观测通道中心波长位于 340, 380, 440, 500, 670, 870, 1020nm，观测时间步长为 15min。NASA 提供的 AERONET 气溶胶光学厚度数据有 3 种: level 1.0 为未经过严格滤云和最后验证的数据; level 1.5 为经过严格滤云但没有最后验证的数据; level 2.0 为经过严格滤云和最后验证、质量有保证的数据。在验证过程中采用质量有保证的二级气溶胶光学厚度数据作为 MODIS_C005 气溶胶光学厚度的验证数据。

2.3 NCEP/NCAR 月平均再分析资料

气象资料选取了 2000—2006 年 NCEP/NCAR 月平均再分析资料，其中包括了 850hp 风场和降雨，利用气象场可以分析气溶胶的传输机制。

3 MODIS 气溶胶产品验证

利用 MODIS_005 气溶胶产品前，先对其在中国海域的适用性进行验证。Hiren 等(2007)在印度利用 MODIS_C005 和 MODIS_C004 气溶胶产品分别与 AERONET 观测值进行比较，发现 MODIS_C005 气溶胶的产品与 AERONET 相关性明显好于 MODIS_C004，更加准确。但在中国海域，MODIS_ C005 气溶胶的产品还没有被验证过。

在验证中，前人大多数研究选取的时空窗口是 50km×50km 和 1 h，但中国海域气溶胶变化很快，具

有局地特征，太大的空间窗口会引入更大的误差，造成验证效果不理想，为了较小误差，通过比较30km×30km, 50km×50km和70km×70km, 3种空间窗口的验证结果，发现30km×30km空间窗口不但可以真实的反映中国海域气溶胶的局地特征，而且大大提高验证效果，真实的反映了卫星数据质量。

图1为4个AERONET陆基观测站的空间分布，它们分别代表了不同海区的情况。图2是各个AERONET站点以及它们总和分别与MODIS_C005在550nm处气溶胶光学厚度使用30km×30km空间窗得到的线性回归分析关系图。从图2中可以看出在各个AERONET站点，MODIS_C005的AOT550与AERONET的AOT550有着很好的相关性，相关系数大于0.9。相关系数最大的Noto站，达到了0.9662。而4个AERONET站的总和与MODIS_C005的相关系数也达到了0.9307，说明在中国海域MODIS_C005的AOT550与AERINET的AOT550有着很好的相关性。同时，NASA规定的误差范围为$\pm0.05\pm0.05\tau$，在每个AERONET站点有超过65%的点在这一范围内，满足设计要求(62%)，说明MODIS_C005的气溶胶产品适用于中国海域。与陈本清等(2005)对台湾海域MODIS_C004气溶胶产品的验证结果比较，MODIS_C005的精度更高，更能准确地反映中国海域的气溶胶状况。

对于小颗粒比例的验证，Anderson等(2005)和Remer(2005)作了大量验证工作，得到了一致的结果，

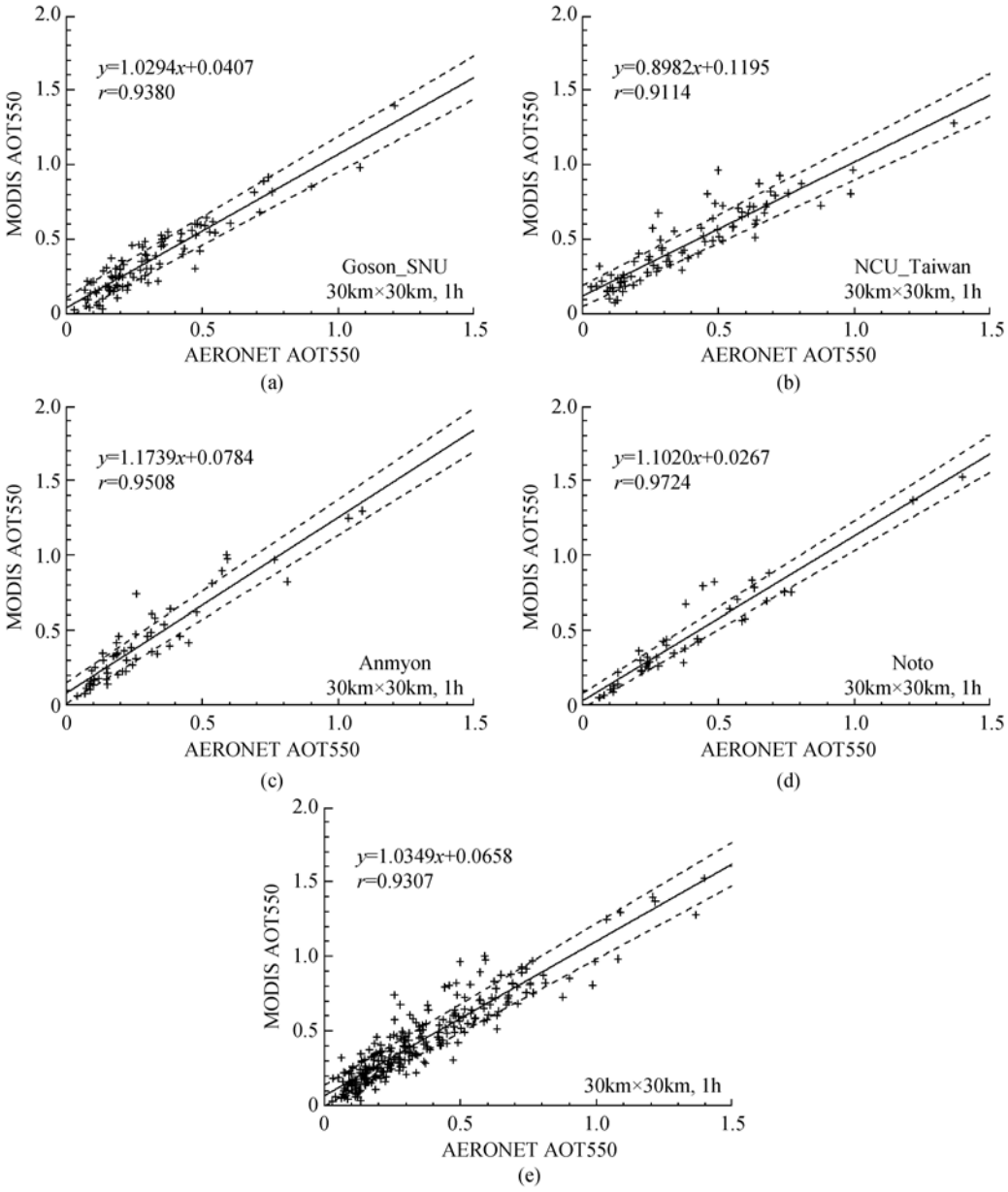

图2 MODIS 550nm气溶胶光学厚度和AERONET 550nm气溶胶光学厚度线性回归分析

(a) Gosan_SNU站; (b) NCU_Taiwan站; (c) Anmyon站; (d) Noto站; (e) 4个站的总和

FMF 在海洋上误差控制在 20%以内。

4 结果分析

4.1 气溶胶光学厚度和小颗粒比例的时间变化

4.1.1 季节变化

图 3 是 2000—2006 年平均的 550nm 气溶胶光学厚度的季节分布。从图 3 可以看出明显的季节变化: 在冬季, AOT550 分布特点是大值区沿着海岸线分布，随着离岸距离增加而减小，在近岸由于人类活动的影响可以达到 0.5 以上，远海在 0.1 左右。在人类活动最为频繁的中纬度，即 30°N 附近 AOT550 达到最大值，在 25°N 以北的海域 AOT550 大于 0.17，在 25°N 以南远离海岸线的海域 AOT550 在 0.1—0.17; 在春季，AOT550 的分布趋势与冬季相似，即沿岸分布。但由于沙尘等要素的影响，整个海区的 AOT550 明显增大，范围也在不断扩大，所有海域的 AOT550 大于 0.17，而且沿着海岸线 AOT550 最大值

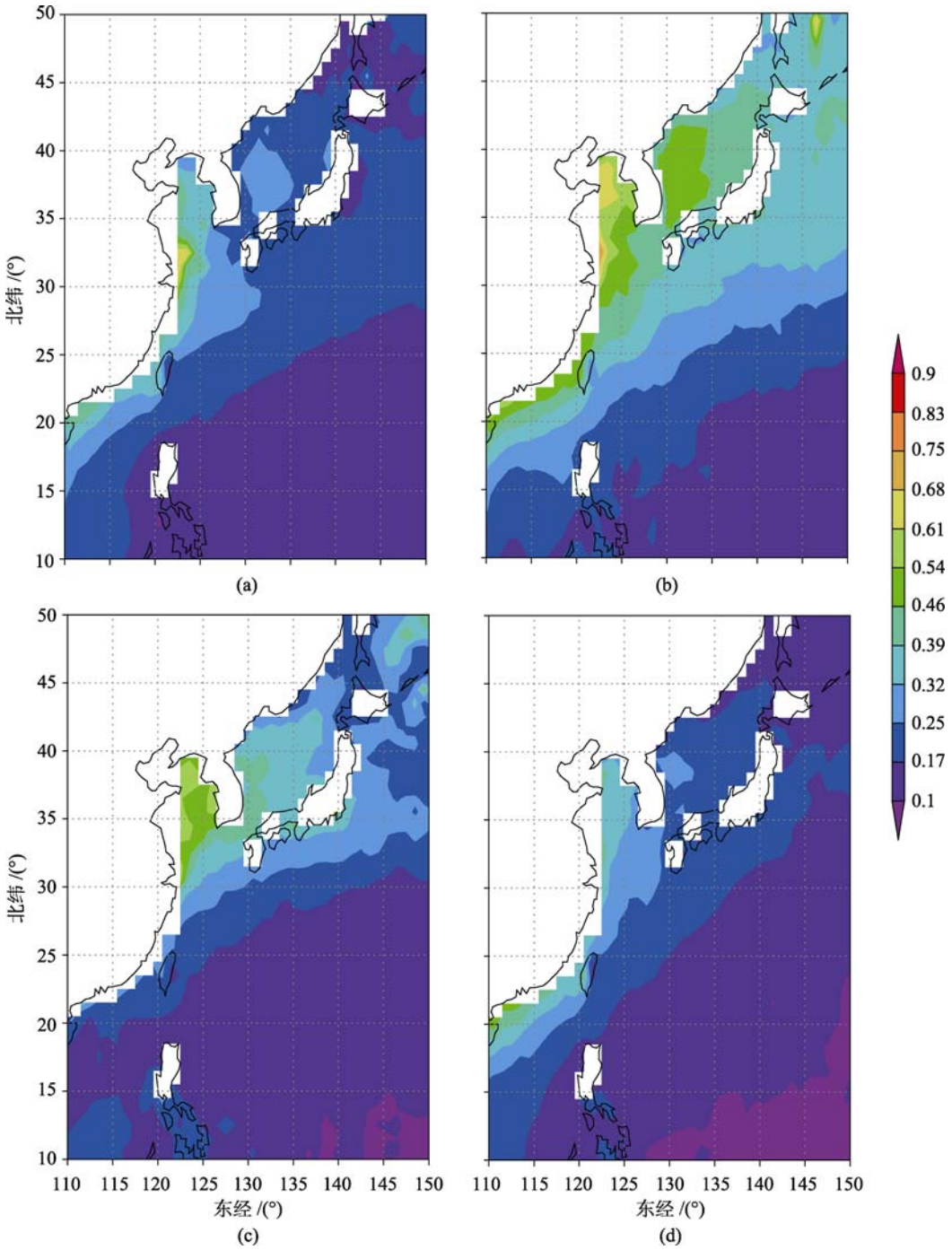

图 3 中国海域 550nm 气溶胶光学厚度(AOT550)的季节分布

(a) 冬季; (b) 春季; (c) 夏季; (d) 秋季

也明显大于冬季。同时在北部海域, AOT550 几乎增加了 1 倍，说明沙尘对于北部的影响更为明显；在夏季, AOT550 的分布发生了显著的变化。主要特点是北部大，南部小。在 30°N 以北，AOT550 保持着冬、春季的分布特点，大值中心出现在黄、渤海海域，其他海域由于降雨等气象条件的改变，AOT550 明显变小。而在 30°N 以南的整个海域，AOT550 明显变小，大部分区域的 AOT550 小于 0.17；在秋季，AOT550 恢复了冬、春的分布特征，但是数值要小于它们，部分海域的 AOT550 甚至小于 0.1。

图 4 是小颗粒比例(FMF)的季节分布。从图 4 可以看出：在冬季，FMF 分布特点与 AOT550 类似，等值线沿海岸线分布，高值区靠近岸边，最大值位于 30°N—35°N，离岸越远，FMF 越小，整个海域的 FMF 大于 0.42，这说明在近岸主要是小颗粒的人为气溶胶为主，随着离岸距离的增加，气溶胶颗粒的尺度是不断增加的，直到远海，气溶胶主要以大颗粒的自然气溶胶为主；在春季，FMF 分布特点和冬季相似，数值相当。在台湾和菲律宾海域以及日本海，由于人类活动增多，FMF 出现了大值区；在夏季，和 AOT550 一样，FMF 的分布发生了很大的变化。除了东南沿海，FMF 在整个海区有不同程度的增大。尤其是在 30°N 以北的大部海域, FMF 明显变大。在黄、渤海区域，FMF 达到最大值，数值达到

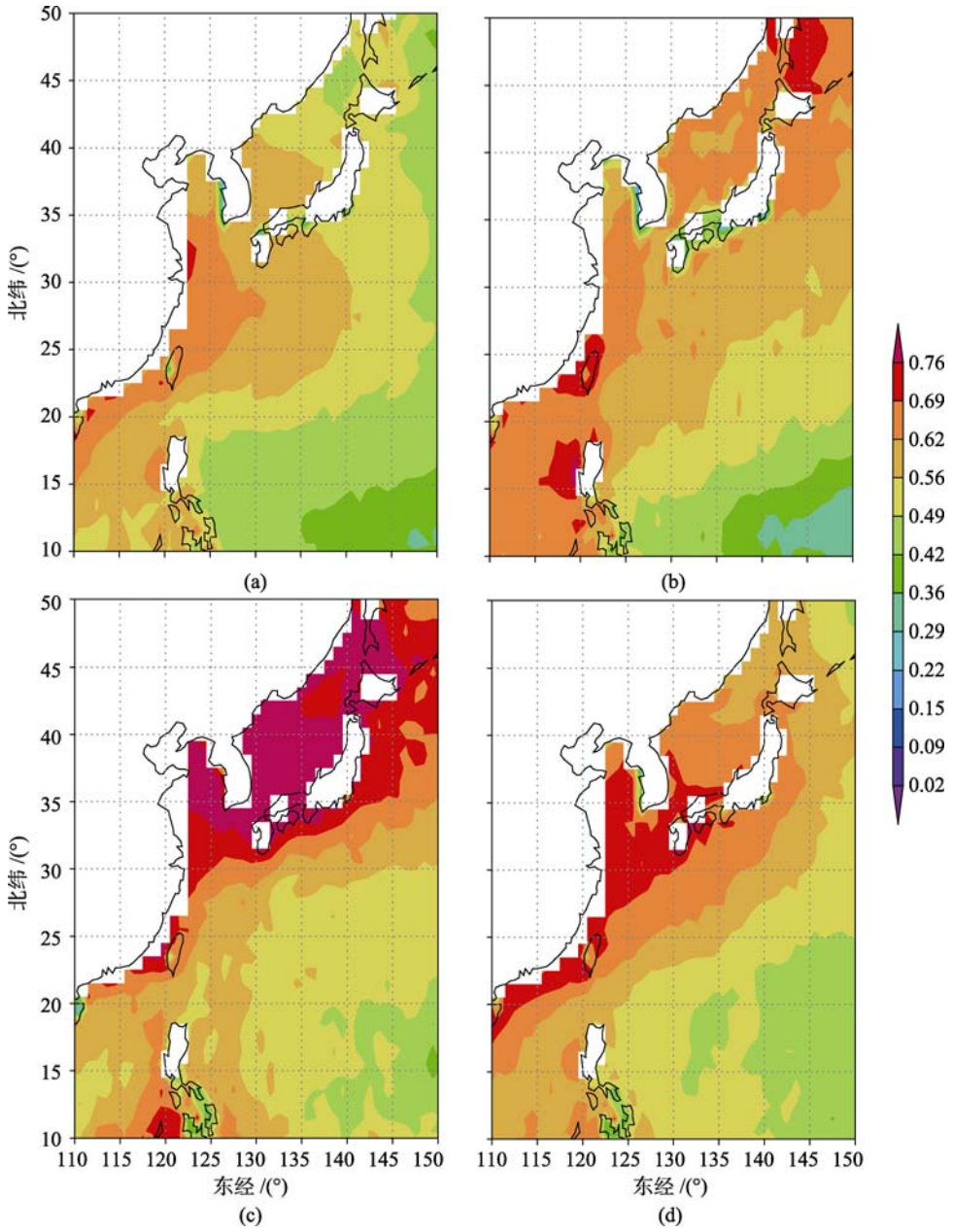

图 4 中国海域小颗粒比例(FMF)的季节分布

(a) 冬季; (b) 春季; (c) 夏季; (d) 秋季

0.8 以上。这说明在夏季，气溶胶主要是由人为气溶胶组成；在秋季，FMF 略有减小，分布也趋于冬季，但数值明显大于冬季。

4.1.2 时间序列

图 5 是中国海域区域平均的时间序列，图 6 是中国海域 6a 区域平均的月变化。图 5 中，AOT550 变化具有很明显的规律，在每年的 3、4、5 月达到最大，而在 10、11、12 月达到最小。从 72 个月的时间序列看，呈现出准一年周期震荡，且在 2 个峰值之间出现单调增或减的趋势；FMF 也同样具有明显的周期变化，在每年的 7、8、9 月达到最大，而在 12 月、次年 1、2、3、4 月达到一年中的最小。在 72 个月的时间序列中也有准一年周期震荡。图 6 中 6a 区域平均的月变化，AOT550 在 1—6 月达到最大，在 7—12 月达到最小，分别在 4 月和 9 月达到极值，呈现正弦分布；同时，FMF 的变化也是很有规律，在 5—10 月达到最大，在 11 至次年 4 月达到最小，在 4 月和 9 月出现极值，与 AOT550 不同， FMF 在 4 月是极小值，在 9 月是极大值，两者位相相反，说明不同种类气溶胶对于总的气溶胶浓度的贡献在每个季节中是不同的。通过以上分析，可以看出中国海域 AOT 和 FMF 存在明显的周期性季节变化。

4.2 气溶胶光学厚度和小颗粒比例的空间分布

中国海域气溶胶不仅存在时间变化特征，同时也具有空间分布的特征。图 7 是 AOT550 和 FMF 在经向和纬向的时空分布。图 8 是 AOT550 和 FMF 在经向和纬向上的 6a 平均变化。从图 7 可以看出，在每一年的冬、春季节，AOT550 在 30°N—40°N 会出现大值区，而同一区域在夏、秋季节 AOT550 则相对较小，说明该区域 AOT550 的季节变化明显。还可以看到在所有季节中，随着纬度从 10°N 向北增加到 30°N，AOT550 逐渐增大，直到中纬度的 AOT550 大值区，反映了一个 AOT550 的经向变化。从图 8 的 6a 区域平均更清楚地看到这点，在 30°N—40°N 出现纬度方向上的大值区，向南北递减，这是由于

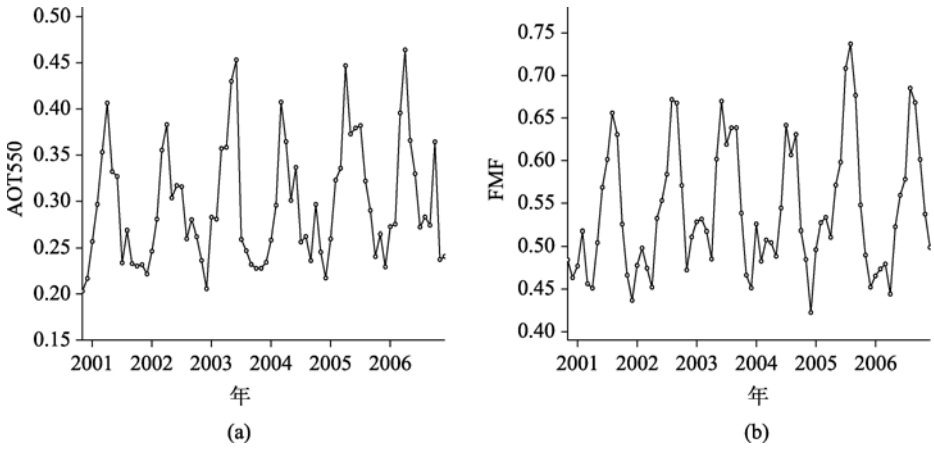

图 5 中国海域区域平均的时间序列

(a) AOT550; (b) FMF

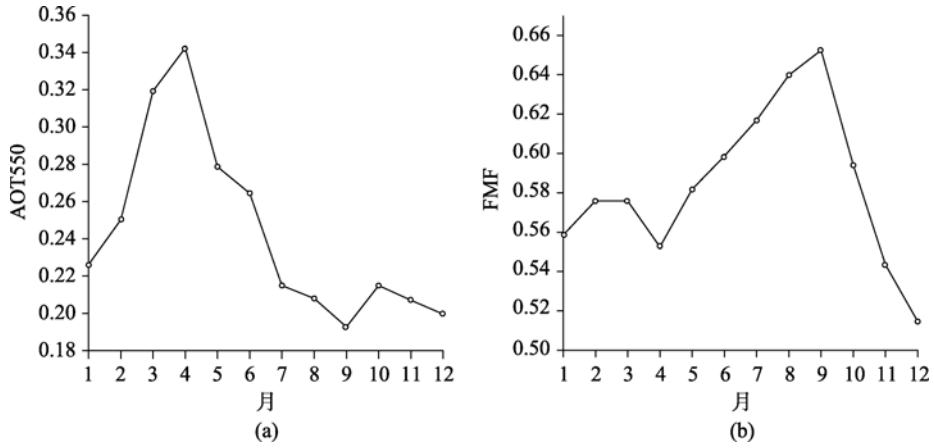

图 6 中国海域 6a 区域平均的月变化

(a) AOT550; (b) FMF

人类活动主要集中在中纬度地区，使这一纬度上AOT550大于其他纬度。同样，从图7中也可以看到FMF的经向变化，FMF的大值区也出现在30°N以北，但FMF的大值区一般出现在夏、秋季节，而冬、春季节相对较小一些。从图8可以看出，对于整个海域的平均，FMF是从10°N增加到30°N，其后一直到40°N比较稳定，说明在30°N区域以北的气溶胶以人为气溶胶为主，该区域的人类活动最为剧烈，FMF比较稳定而且更加接近，而低纬度人为气溶胶不占据主导地位，随着纬度减小，人类影响越来越弱，造成FMF随纬度减小的趋势。

经向上，它们的变化更加明显。图7中在120°E—123°E，所有时间段有一个AOT550的大值区，这是因为中国的大部分沿海区域在120°E—123°E这个范围内，这个海域受人类影响最为严重，所以AOT550常年很大。从图8看经向的变化更明显，随着经度从120°E开始增加，AOT550不断减小，反映了人类活动对海洋气溶胶的影响随着离岸距离增加不断的减弱。再看FMF，它的经向变化和AOT550类似。在近岸，也就是125°E以西FMF很大，说明人类活动作用明显，气溶胶主要以人为气溶胶构成。随着经度不断向东，人类活动的痕迹越来越小，这主要表现在FMF减小，说明了中国海域气溶胶受人类活动的影响是非常严重的。图8中FMF的6a的区域平均也说明了这一点，随着经度不断的东移，FMF不断减小。

4.3 原因分析

通过上面分析可以看出，中国海域气溶胶存在着显著的时空分布特征，我们主要从传播机制进行分析。

陆源气溶胶通过一定的条件到达海洋上空，借

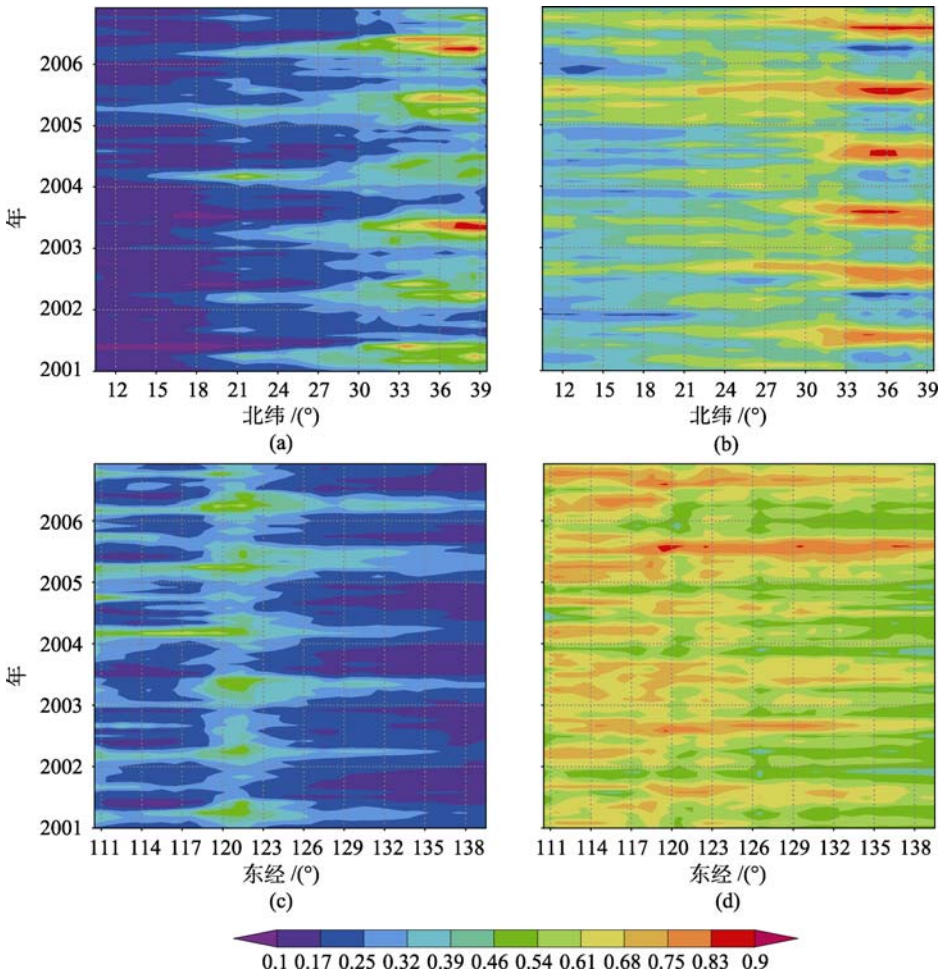

图7 中国海域AOT550和FMF的经纬向分布图

(a) 纬向AOT550; (b) 纬向FMF; (c) 经向AOT550; (d)经向FMF

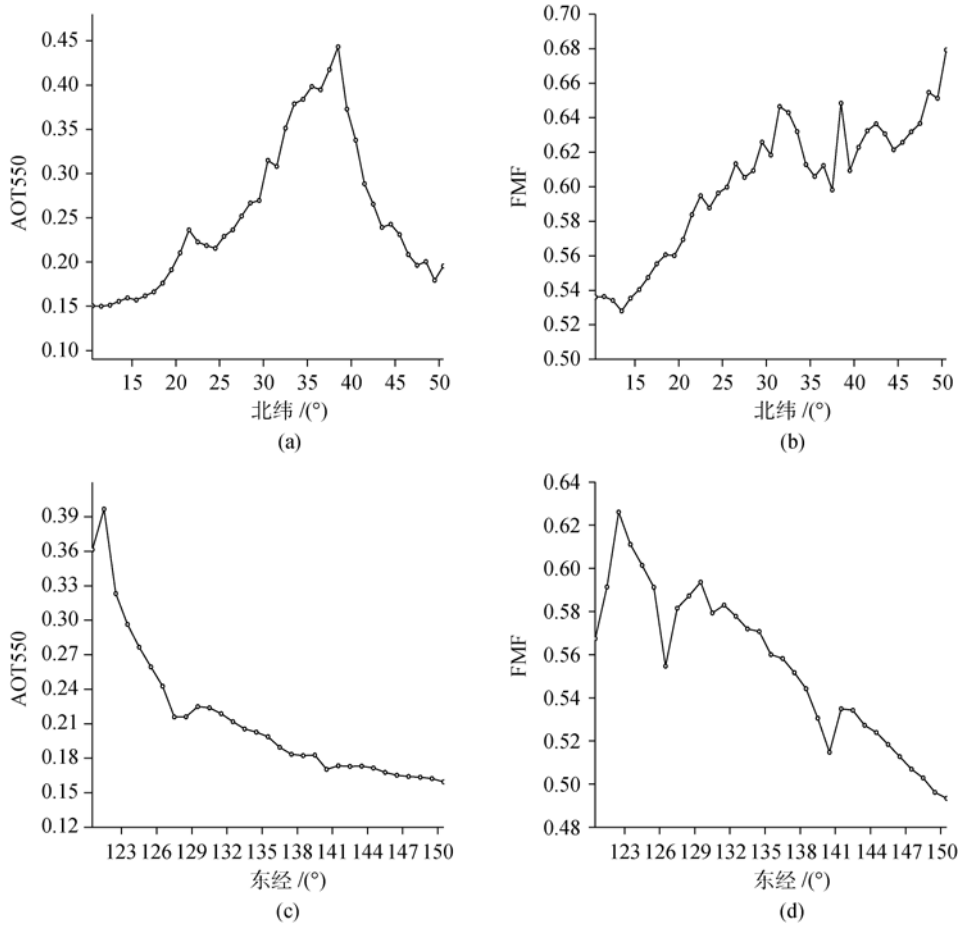

图 8 中国海域 6a 区域平均的经纬向变化

(a) 纬向 AOT550; (b) 纬向 FMF; (c) 经向 AOT550; (d)经向 FMF

助于气象场分析。图 9 是 2000—2006 年 6a 的 850hp 风场的季节平均。可以看出，冬、春季风场分布类似，在 20°N 以北被西北风控制，在 20°N 以南被平直的东风控制。夏、秋季，大部海域被东风控制，只有 30°N—40°N 的小部分地区存在西南风。至于 4 个季节的降雨，则是夏季最大，秋季次之，冬春最小。这种气象场的分布决定了中国海域气溶胶的分布。

冬季, 20°N 的西北风把陆源气溶胶输送到海上，但海上的西风风速明显大于陆地上，在 4 个季节里也是最大的，这就造成陆源气溶胶到达中国海域后很快就被继续向东输送，并未产生堆积，使得冬季的中国海域 AOT550 并未达到最大值。同时由于海上风速大，造成大颗粒的海盐气溶胶的大量产生，使得 FMF 达到一年中的最小；春季，由于北方沙尘和沿海工业排放的共同作用，借助西北风的输送，大量的气溶胶到达中国海域，同时由于风速的减小和沙尘等大颗粒气溶胶的存在，有利于气溶胶粒子在中国海域的堆积，使其 AOT550 达到一年的最大。同时，大量沙尘气溶胶的注入，使得 FMF 也很小，仅次于冬季；夏季，大部海域是东风，这一风场分布不利于陆源气溶胶向海输送，所以 AOT550 出现一年中的最小值。而且夏季降雨一年中最多，把大量的大颗粒气溶胶清除，小颗粒气溶胶比例增加，所以 FMF 达到一年中的最大值；秋季，大部海域依然是被东风控制，在 30°N 以北的沿海出现了很弱的西风，使得中纬度沿海出现了 AOT550 的增加。同时秋季的降雨量仅次于夏季，所以它的 FMF 也很大，只比夏季小，比冬春季大。总之，AOT 和 FMF 的时空分布和气象场有非常紧密的关系。

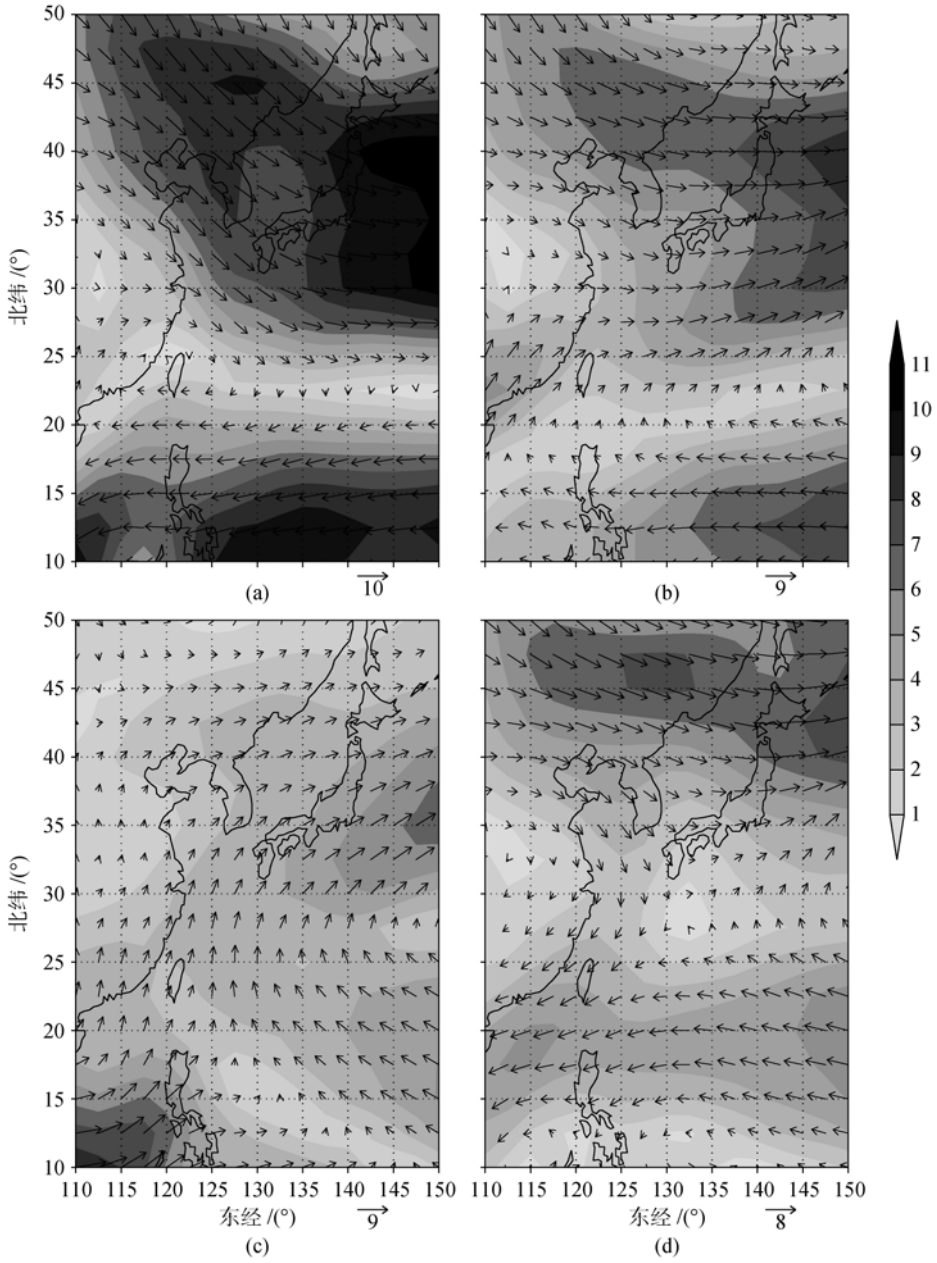

图 9　中国海域 2000—2006 年 6a 的 850hp 风场的季节平均

(a) 冬季; (b) 春季; (c) 夏季; (d) 秋季

5　结　论

通过 AERONENT 地基观测，对 MODIS_C005 气溶胶产品在中国海域的适用性进行了验证；并利用 MODIS_C005 气溶胶产品对中国海域气溶胶的分布进行了分析；最后结合气象场，探讨了其形成机制。得到以下主要结论:

(1)通过于 AERONENT 地基观测相比较，发现 MODIS_C005 气溶胶产品在中国海域具有很高的精度，满足 NASA 的设计要求，适用于中国海域。

(2)中国海域气溶胶光学厚度(AOT550)与尺度分布(FMF)存在着明显的季节变化。AOT550 在冬、春季最大，在夏、秋季最小；而 FMF 在夏、秋季达到最大，在冬、春季达到最小。同时它还存在准一年的周期震荡。

(3)中国海域 AOT 和 FMF 存在显著的空间分布特征。纬向上, AOT550 在 30°N—40°N 达到最大，向南北递减; FMF 从南向北逐渐增加，到达 30°N 附近后增加减弱。经向上，AOT550nm 和 FMF 是随着经度的增加而减小的，说明陆源人为气溶胶是影响中国海域气溶胶的重要因素。

(4)结合气象场分析，发现借助风场传输，陆源气溶胶到达中国海域，同时还受到降雨的影响。

致 谢 本文使用了 NASA GSFC 提供的 MODIS Leve12 和 Leve13 数据，以及 AERONET 观测网的气溶胶产品，在此表示感谢。

REFERENCES

Anderson T L, Wu Y and Chu D A. 2005. Testing the MODIS satellite retrieval of aerosol fine-mode fraction. *J. Geophys. Res*., **110**: 182—193

Bellouin N, Jones A and Haywood J. 2008. Updated estimate of aerosol direct radiative forcing from satellite observations and comparison against the Hadley Centre climate model. *J. Geophys. Res*., **113**: 1043—1546

Cheng B Q and Yang Y M. 2005. Validation of MODIS aerosol optical thickness in the Taiwan Strait and its circumjacent sea area. *Acta Oceanologica Sinica*, **27**(6): 170—176

Christopher S A, Gupta P and Haywood J. 2008. Aerosol optical thicknesses over North Africa: 1. Development of a product for model validation using qzone monitoring instrument, multiangle imaging spectroradiometer, and aerosol robotic Network. *J. Geophys. Res*., **113**: 1446—1457

Hao Z Z, Pan D L and Bai Y. 2007. Characteristics of the spatial distribution and monthly variation of aerosol optical thickness derived from SeaWiFS over the China Sea. *Journal of Marine Sciences*, **25**(1): 80—87

Hiren J, Satheesh S K and Srinivasan K. 2007. Assessment of second-generation MODIS aerosol retrieval(Collection 005) at Kanpur, India. *Geophysical Research Letter*, **34**: 1902—1918

Holben B N, Eck T F and Slutsker I. 1998. AERONET-A federated instrument network and data archive for aerosol characterization. *Remote Sensing of Environment*, **66**: 1—16

Li X W, Zhou X J and Li W L. 1995. The cooling of Sichuan province in recent 40 years and its probable mechanism. *Acta Meteorologica Sinica*, **9**: 57—68

Li Z Q, Zhao F S and Zhao W. 2003. Ground surface observationof aerosol optical thickness over Yellow Sea region. *Chinese Journal of Quantum Electronics*, **20**(5): 635—640

Menon S, Hansen J and Nazarenko L. 2002. Climate effects of black carbon aerosols in China and India. *Science*, **297**: 2250—2253

Patadia F, Gupta P and Christopher S A. 2008. First observational estimates of global clear sky shortwave aerosol direct radiative effect over land. *Geophys. Res. Lett*., **35**: 348—360

Remer L A. 2005. The MODIS aerosol algorithm, products and validation. *J. Atmos. Sci*., **62**: 947—973

Remer L A and Kaufman Y. 2005. Didier Tanre. Collection 005 change summary for MODIS aerosol(04_L2) algorithms. USA: NASA

Zhang C C and Zhou W X. 1995. The Lecture of Atmospheric Aerosol. Beijing: China Meteorological Press

Zhang X Y. 2007. Aerosol over China and their climate effect. *Advances in Earth Science*, **22** (1): 12—16

Zhao C S, Tie X X and Lin Y P. 2006. A possible positive feedback of reduction of precipitation and increase in aerosols over eastern central China. *Geophys. Res. Lett*., **33**: 118—132

Zhao W, Tang J W and Gao F. 2005. Measurement and study of aerosol optical properties over the Huanghai Sea and the East China Sea in the spring. *Acta Oceanologica Sinica*, **27**(2): 46—53

附中文参考文献

陈本清，杨燕明. 2005. 台湾海峡及周边海区 MODIS 气溶胶光学厚度有效性验证.海洋学报, **27**(6): 170—176

郝增周，潘德炉，白雁. 2007. SeaWiFS 遥感资料分析中国海域气溶胶光学厚度的季节变化和分布特征. 海洋学研究，**25**(1): 80—87

李正强，赵凤生，赵崴. 2003. 黄海海域气溶胶光学厚度测量研究. 量子电子学报, **20**(5): 635—640

张小曳. 2007. 中国大气气溶胶及其气候效应的研究. 地球科学进展, **22**(1): 12—16

章澄昌，周文贤. 1995. 大气气溶胶教程.北京：气象出版社

赵崴，唐军武，高飞. 2005. 黄海、东海上空春季气溶胶光学特性观测分析. 海洋学报, **27**(2): 46—53